Journal of Applied Polymer Science

Vertically Aligned Carbon Nanotube-Based Composite: Elaboration and Monitoring of the Nanotubes Alignment

Mickael Huard,[1] Florent Roussel,[2] Stéphan Rouzière,[1] Stéphanie Patel,[2] Mathieu Pinault,[2] Martine Mayne-L'Hermite,[2] Pascale Launois[1]

[1]Laboratoire de Physique des Solides, UMR CNRS 8502, Université Paris Sud 11, 91405 Orsay Cedex, France
[2]Laboratoire Francis Perrin - CEA CNRS URA 2453, CEA Saclay, 91191 Gif-sur-Yvette Cedex, France
Correspondence to: P. Launois (E-mail: pascale.launois@u-psud.fr)

ABSTRACT: We present the different elaboration steps of a composite formed of carbon nanotubes (CNT) carpet embedded in an epoxy polymer. Detailed characterization at each step of the elaboration process is performed. The good alignment of CNT in as-grown carpets is kept all along the elaboration process of the composite, as it is measured at both macro and microscopic scales by X-ray scattering. We also ensured by X-ray fluorescence measurements that the iron-based catalyst particles used for the synthesis were removed from the carpet after a high temperature post-annealing treatment. These measurements give valuable information for further applications involving unidirectional nanotube composites and membranes, where CNT alignment is a key parameter. © 2013 Wiley Periodicals, Inc. J. Appl. Polym. Sci. **2014**, *131*, 39730.

KEYWORDS: composites; nanotubes; graphene and fullerenes; X-ray; membranes; microscopy

Received 30 April 2013; accepted 3 July 2013
DOI: 10.1002/app.39730

INTRODUCTION

Arrays of vertically aligned carbon nanotubes (VACNT) are promising carbon nanostructure networks allowing to prepare new multifunctional materials for a variety of potential applications such as interconnects,[1] membranes for separation or filtering,[2] composites for aerospace applications,[3] or sensors.[4] VACNT form macroscopic samples free from amorphous carbon and exhibiting a rather narrow range of nanotube lengths and diameters, as well as well-defined large surface area, which enable to readily incorporate them into device or multifunctional material configurations. In addition, such aligned networks are porous, and it is necessary to consolidate them by a matrix which is infiltrated inside, giving rise to a composite material. Several studies are reported in the literature regarding the resulting properties of such composite and claiming that the enhancement of properties is due to the anisotropy of such CNT networks. For instance, it is found that for anisotropic composites containing aligned multi-walled carbon nanotubes embedded in epoxy or silicone, the electrical resistivity and the mechanical properties are higher in the axial direction of CNT as compared to the transversal direction.[3,5–8] Thermal properties are also improved in the axial direction of CNT in VACNT/polymer or pyrocarbon composites.[9–11]

Generally, processing of VACNT is carried out by incorporating polymers,[12] ceramics,[13] or carbon[11] in the inter-tube free space in order to transform them into a suitable composite material for the required application. Different processing techniques have been developed such as in-situ injection molding,[12] infusion of aerospace-grade epoxy polymers into VACNT via capillary-induced wetting,[3,8] infiltration into VACNT of monomers followed by in-situ polymerization[14–16] or incorporation of polymer solutions into VACNT networks.[2,17] For all these composites, the alignment of carbon nanotubes is of high importance since this is one of the key factors to optimize the properties. Nowadays, from the literature, such infiltration process seems to be acquired but since such process needs, most of the time, to use a liquid phase which could involve a shrinkage of the aligned CNT network during the drying step and therefore a misalignment of CNT. It is then crucial to study precisely the potential changes of the alignment degree along the different steps of the fabrication process. Indeed, according to the processing route, the alignment of CNT can be significantly modified during the different preparation steps. However, only few studies report the quantitative characterization of the alignment degree before and after VACNT processing. Characterization of the alignment reported in studies related to the preparation of VACNT/polymer composites is generally performed by Scanning Electron Microscopy (SEM), giving only qualitative information on the alignment of CNT in composite samples. Few works have attempted to quantify the alignment degree of CNT before and after the composite fabrication, by

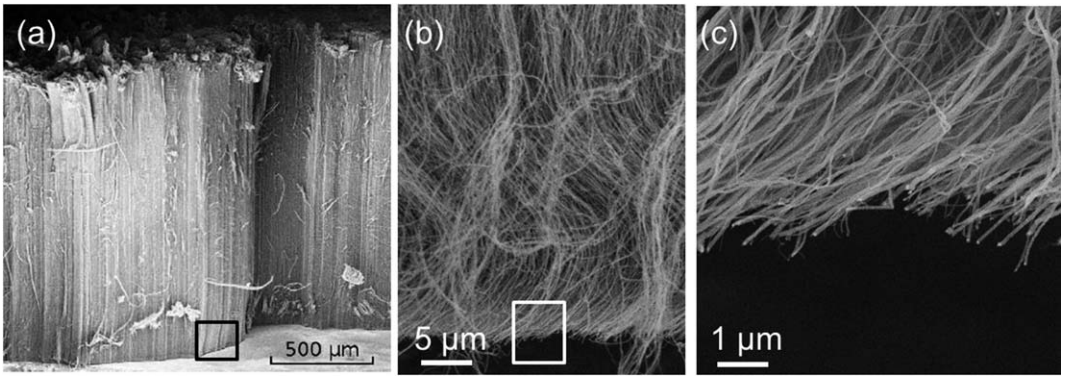

Figure 1. SEM observations of (a) the raw vertically aligned MWCNT carpet after the synthesis, (b) the misaligned area at the carpet base (part of the selected area in (a)) induced by its separation from the quartz substrate using a razor blade, (c) magnification view of the selected area in (b).

using either polarized Raman spectroscopy[15] or Small Angle X-Ray Scattering.[3,8] In the first case, the similar alignment degree between raw VACNT and VACNT/PMMA composites allows to conclude that the PMMA infiltration process from MMA monomer does not induce modification of the CNT alignment.[15] However, typical volume probed with Raman scattering is only ~1 μm^3. In the second case, SAXS measurements demonstrate that the alignment is preserved in epoxy–CNT composite. Those experiments are macroscopic (larger beam size and penetration length than Raman), but they were performed using synchrotron radiation, which cannot be used for routine measurements of the alignment degree during the composite preparation process.

In this context, the objective of our study was to measure the alignment degree of CNT after each step of the elaboration process of VACNT/epoxy composite materials using an epoxy polymer solution, on a laboratory set-up, available for routine characterization. Note that an important step preliminary to the incorporation of polymer is the annealing treatment of VACNT carpets, grown by aerosol-assisted Catalytic Chemical Vapor Deposition (CCVD), allowing removal of metal catalyst-based nanoparticles confined into CNT.[18] According to the expected application, in the case of filtration membranes[2] for instance, measurement of the iron content after this annealing step is of high importance. Our measurements, performed by X-ray micro-diffraction, enable us to follow the alignment degree of CNT all along the VACNT height, at each step of the composite elaboration process. In addition, X-ray micro-fluorescence is used to determine the occurrence of metal catalyst traces all along the VACNT height. Such measurements are crucial for the control of the composite preparation. It makes it possible to select the area in the final VACNT–polymer network exhibiting the highest and constant CNT alignment degree and no metal catalyst-based by-products.

EXPERIMENTAL

Synthesis and Impregnation

Large carpets (1.5 × 1.5 cm^2) made from vertically aligned multi-walled carbon nanotubes (MWCNT) were synthesized by aerosol-assisted CCVD process.[19] Toluene and ferrocene were injected under argon flow for 75 min on quartz substrates placed in a reactor heated at 850°C. The first step of the elaboration process corresponds to the synthesis of well-aligned carbon nanotube carpets and enables to get raw carpets. They are removed from their quartz substrate on which they grew using a razor blade. This mechanical separation of the carpet leads to a misalignment of the base of the carpet on approximately 10 μm as seen in Figure 1. The second step is an annealing treatment of raw samples at 2000°C for 2 h in an inert atmosphere of argon, in order to improve their structural quality and remove iron nanoparticles encapsulated inside the nanotubes.[18] The third step is the preparation of unidirectional composite materials from annealed carpets (Figure 2). The process consists in infiltrating a solution of epoxy polymer in the inter-tube space (around 80–100 nm). The epoxy solution is made from a commercial mixture composed of a resin (Epon: Epon 812 substitute), a hardener (MNA: Methyl-5-norbornene-2,3-dicarboxylic anhydride [$C_{10}H_{10}O_3$]) and an accelerator [DMP30: (2,4,6-Tris(dimethylaminomethyl) phenol ($[(CH_3)_2NCH_2]_3C_6H_2OH$)]. In order to ensure an efficient filling of the solution mixture in the inter-tube space, and therefore a subsequent homogeneous curing of the polymer between nanotubes (key step to be controlled in order to avoid the presence of too important remaining porosity), several degassing cycles were performed to remove the air entrapped in the inter-tube porosity.

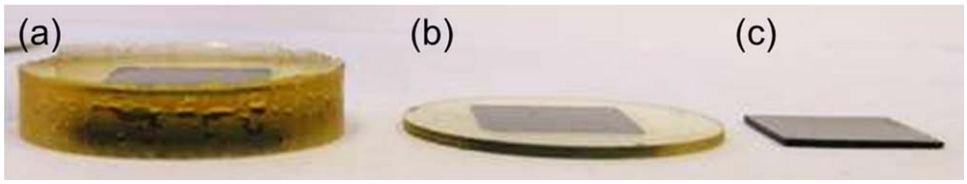

Figure 2. Composite material sample, (a) after embedding with epoxy; (b) after polishing; (c) composite with the surrounding polymer removed. [Color figure can be viewed in the online issue, which is available at wileyonlinelibrary.com.]

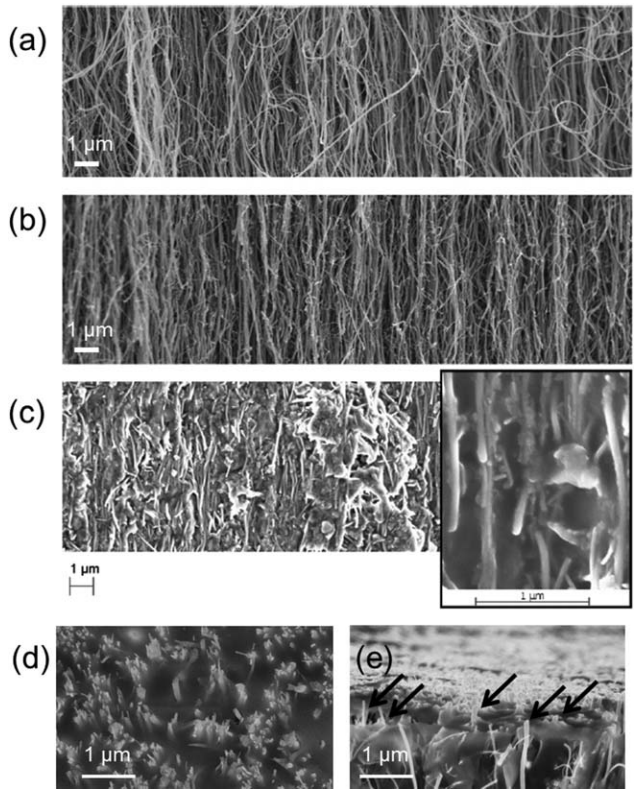

Figure 3. SEM observation of the VACNT carpets: cross sections of (a) raw carpet, (b) annealed carpet, and (c) embedded carpet. (d,e): SEM observations of the polished surface of the composite, respectively, obtained above the composite top surface and on the top cross section of the composite, allowing to distinguish the CNT protruding from the polymer surface (arrows). Same observations have been made (not represented) on the bottom surface of the composite.

A curing treatment at 60°C for 4 days was then carried out. The resulting material is formed of the embedded aligned CNT network, with excess polymer all around, as shown on Figure 2(a). A first thinning step by mechanical polishing is performed and allows us to remove the excess of polymer surrounding the VACNT carpet [Figure 2(b)]. Finally, a second mechanical polishing step is performed which results in the final composite material exhibiting a controlled thickness as shown on Figure 2(c). Note that during this mechanical polishing step the misaligned bottom part of the carpet (Figure 1) is removed.

SEM Analysis

All the processing steps used to elaborate the composite could affect the initial alignment degree in the VACNT carpets. Our objective was to keep the good alignment degree of the raw carpets at all the elaboration steps of the 1D CNT/epoxy composite, especially during the impregnation of the epoxy resin through the aligned CNT network. After each fabrication step, samples were observed by SEM (FEGSEM, Carl Zeiss Ultra 55).

Raw and annealed VACNT carpets exhibit a *ca.* 1.15 mm thickness. Almost no by-products outside nanotubes except on top part of the carpet can be observed, and nanotubes clearly appear preferentially aligned perpendicularly to the carpet base, as shown on Figure 3(a) and (b). They look continuous from the bottom to the top of the carpet. Transmission Electron Microscopy (TEM, Philips CM12) was performed on raw and annealed samples previously dispersed in ethanol, in order to determine their diameter distribution. For both raw and annealed samples, the mean internal and external diameters are 8 and 45 nm, respectively. Considering the CNT carpet weight (52 mg) and the density of CNT (2 g/cm^3), the CNT volume fraction in these samples is *ca.* 10% with a density in nanotubes of 6×10^9 CNT/cm^2.

Regarding composites, SEM observation of the polished cross section of composite [Figure 3(c)] reveals that carbon nanotubes are embedded in the polymer from the top to the base of the carpet, attesting that epoxy is impregnated all along the carpet height. The content of epoxy inside the composite has been determined by thermo gravimetric analysis (TGA, Netzsch apparatus) under flowing argon up to 700°C (heating rate: 10°C min^{-1}). TGA was performed on composite sample and compared to the one of raw VACNT carpet and epoxy resin (Figure 4). From these data, the ratio in mass between the epoxy resin and the carbon nanotube is found to be equal to 2.85.

SEM observations [Figures 3(d,e)] of the polished surface of the composite allow one to visualize the extremities of the nanotubes on both faces of the 1D CNT/epoxy composite and show that the CNTs are protruding from the polymer by a few nanometers [arrows on Figure 3(e)]. Such observations allow one to infer that vertical CNT in the carpet did not lied down during the elaboration of the composite. However, the insulating polymer all around nanotubes is a limiting factor for the clear observation of the nanotubes alignment in such composites. Moreover, SEM gives only qualitative information about CNT alignment. Therefore, it is important to quantitatively determine the alignment degree of CNT after the different steps of the elaboration process of composites.

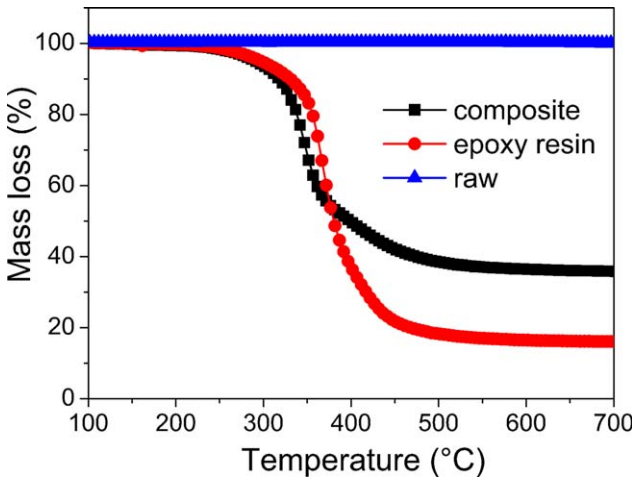

Figure 4. TGA analysis under argon atmosphere of the raw VACNT carpet, epoxy resin, and composite. [Color figure can be viewed in the online issue, which is available at wileyonlinelibrary.com.]

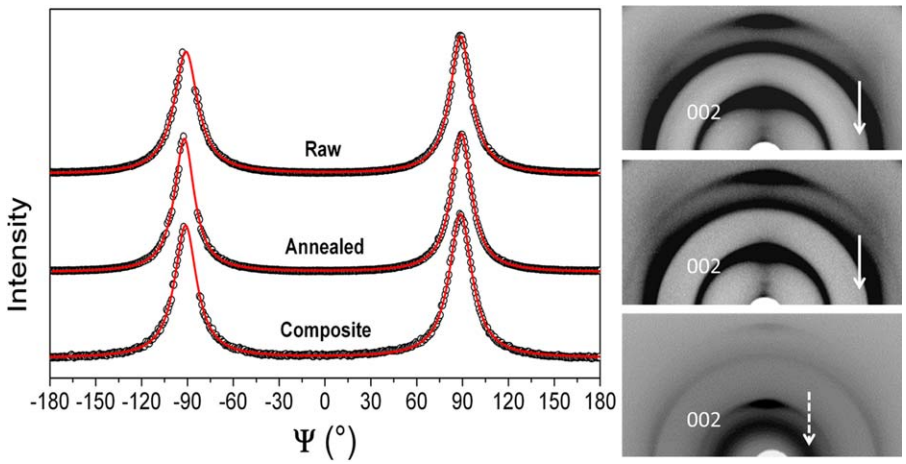

Figure 5. Left: angular intensity variation of the 002 peak as a function of the azimuthal angle at each step of the process. The points are the data and the red curves are Lorentzian fitting functions (HWHM ∼ 8.5°). Right: corresponding X-ray scattering patterns. White arrows show the position of a diffraction ring from cementite, present in the raw sample and absent in the annealed one. Dashed white arrow points towards diffuse scattering from the epoxy polymer in the composite. The 004 peak is at the higher wave vector and the 10 ring is shifted between 002 and 004 ones. [Color figure can be viewed in the online issue, which is available at wileyonlinelibrary.com.]

X-ray Scattering and X-ray fluorescence: Experimental

Two series of X-ray scattering experiments have been carried out on laboratory rotating-anode generators, in transmission, on three samples corresponding to the three steps of the elaboration of composites: raw carpets, annealed carpets, and CNT-epoxy composites. Measurements were performed on the carpets after they had been separated from their quartz substrate on which they grew using a razor blade, since the substrate would hinder the observation of the X-ray scattering signals coming from the carpets. The geometry of the experiments is the same as described in Refs. [20,21]. The incident X-ray beam is perpendicular to the CNT long axis and scattering pattern is recorded on a two-dimensional detector placed behind the sample. Macroscopic scale measurements are performed with a millimetric size beam at 17.4 keV to get global information averaged on a large part of the studied sample. Data are recorded on two-dimensional Imaging Plate. Microscopic scale measurements are performed with a 20 μm size beam at 8 keV on a specially designed set-up.[22] This prototype instrument has been developed to allow the simultaneous acquisition of both X-ray scattering and X-ray fluorescence data at a microscopic length scale for mapping studies on materials. Collimation is achieved with a multilayer optics and a pinhole system. A 2D direct-illumination CCD detector allows one to measure weak scattered signals, while chemical analysis is performed in parallel with an X-ray fluorescence detector. Measurements along the height of the sample are performed thanks to a motorized translation stage, with a 20 μm step. X-ray microdiffraction patterns allow one to probe nanotubes alignment at different heights, while the fluorescence analysis is used to determine the presence or not of iron-based nanoparticles in the sample.

RESULTS AND DISCUSSION

CNT Alignment

The alignment of CNT in the carpet or in the final composite material is given by the anisotropic angular distribution intensity of the 002 diffraction ring at $Q = 1.83\text{Å}^{-1}$, which is related to the inter-wall distance in the multi-walled carbon nanotubes. Note that for a nanotube powder, the intensity would be constant over this ring. The 002 and 004 peaks of the raw and annealed carpets and of the composite are measured on the X-ray scattering patterns in Figure 5. The 10 ring, corresponding to the hexagonal network of the aligned nanotubes, is also clearly visible. We note here that the epoxy polymer diffusion at lower wave vector does not mask the 002 peak from MWCNT.

Previous works have shown that the angular distribution of the 002 ring is related to the orientation distribution function of the nanotubes in direct space.[20] For the three samples (raw carpet, annealed carpet, and composite), angular intensity modulations are well fitted with Lorentzian functions with the same Half-Width at Half-Maximum (HWHM ∼ 8.5°). It corresponds[23,24] in real space to an orientation distribution function which is a Lorentzian$^{3/2}$, with HWHM $w_d \sim 6.5°$. In the three samples, the nanotubes are thus mainly aligned along the normal of the growth substrate within 6.5°. This preservation of the CNT alignment from the raw carpet to the final composite is an important result, since the alignment of the nanotubes is a key point for applications.

Micro-diffraction measurements were also performed after each step of the composite elaboration, bringing information on the CNT alignment along the height of the carpet. Micro-beam (20 μm diameter) being less intense than the standard one (1 mm diameter) used before, absorption of part of the scattered signal by the epoxy polymer makes the analysis more difficult for the composite. However, our microdiffraction measurements allowed us to determine locally the nanotubes alignment in the three samples, as shown in Figure 6. First, one finds that the evolution of the alignment degree versus the beam position is very similar whatever the elaboration step, demonstrating that the process does not alter the CNT alignment. Moreover, in all samples, alignment is slightly worse at the top and at the base

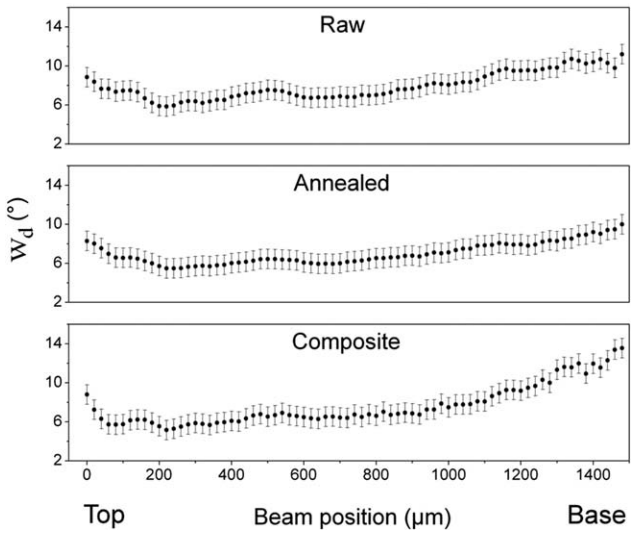

Figure 6. Evolution of nanotubes orientation, measured by micro-diffraction, along the height of the raw carpet, the annealed carpet, and the composite (top and base of the samples are indicated, the base corresponding to the area initially in contact with the substrate on which the carpet grew); w_d is the half-width at half maximum of the nanotubes orientational distribution function (see in the text).

of the carpet than in the middle of the carpets. The poorer alignment at the base of the carpet is mostly caused by the mechanical separation of the carpet from the substrate, the razor blade bending the nanotubes. On the top of the carpet, which corresponds to the beginning of the carpet growth (base growth mechanism),[19] nanotubes are less dense, entangled, and alignment is poorer. However, with our method, we can identify a large region where the orientation is optimum and quite constant. In the perspective of future applications such as membranes, it will thus be possible to select the adequate zone to keep before the final thinning step.

Control of Iron Removal

The 121/210 diffraction peaks from Fe_3C cementite, at very close wave-vectors, not resolved in our experiments, are shown in Figure 5 by a white arrow on the raw carpet pattern. Cementite is found at the carpet base and encapsulated inside the nanotubes during their growth.[25] Its diffraction peaks are no more visible on the scattering pattern of the annealed sample, indicating that cementite nanoparticles have been removed during the annealing step. The same result holds for other iron-based nanoparticles present in the raw carpet, such as γ-iron.[26] However, if amorphized, iron nanoparticles would no more be visible in diffraction experiment. Moreover, particles smaller than ~5 nm, possibly present outside the tubes, especially at the top of the carpet, as discussed below, would not be observed by X-ray diffraction. We thus performed X-ray fluorescence measurements with the 20 μm beam size setup. Iron fluorescence signal along the height of the raw and annealed carpets is shown in Figure 7. Excess of iron at the basis of the raw carpet corresponds to the catalyst particles, as shown in previous work.[21] Excess of iron at the top of the carpet is the result of phenomena occurring during CNT growth: the top part of the carpet is in direct contact with iron based catalyst particles which are formed in the gas phase from ferrocene decomposition[27] and are subsequently trapped on the top surface of the carpet. No iron fluorescence signal is observed in the annealed sample. This measurement demonstrates that iron has not been amorphized during the annealing step but that iron-based nanoparticles, whatever their size, have indeed been removed.

CONCLUSIONS

The alignment of the carbon nanotubes in composites being an essential parameter for applications, it is crucial to ensure that it is not modified during the successive steps of the composite fabrication. We report here that the orientation distribution of the carbon nanotubes remains the same, all along the carpet height, from the raw carpet to the final epoxy–VACNT composite we elaborated. This study validates the impregnation technique used to prepare the composites. It also allows selection of the better aligned portions of the composite for further thinning procedures. All techniques, electron microscopy, but also X-ray diffraction and X-ray fluorescence, are used in laboratory and are thus available for routine characterization.

ACKNOWLEDGMENTS

The authors thank J. Cambedouzou and V. Heresanu for their active participations in preliminary experiments. This study has been partially supported by the French National Agency (ANR) in the frame of its technological Research NANO-INNOV/RT

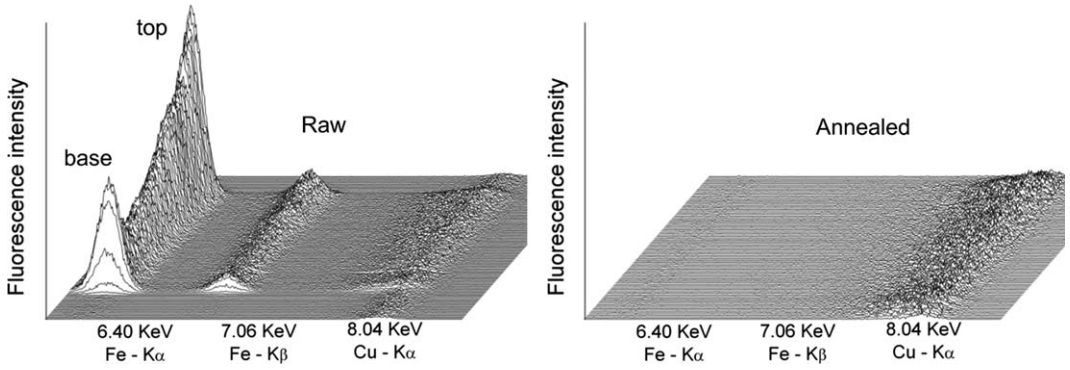

Figure 7. Fluorescence signal along the raw and annealed carpet height. Both K_α and K_β fluorescence peaks of iron are clearly visible for the raw carpet. The weak Cu contribution comes from the experimental set-up.

program (NawaA4, project No.ANR-09-NIRT-005-01), and by C'Nano Ile de France.

REFERENCES

1. Esconjauregui, S.; Fouquet, B.; Bayer, C.; Ducati, C.; Smajda, R.; Hofmann, S.; Robertson, J. *ACS Nano* **2010**, *4*, 7431.
2. Hinds, B. J.; Chopra, N.; Rantell, T.; Andrews, R.; Gavalas, V.; Bachas, L. G. *Science* **2004**, *303*, 62.
3. Wardle, B. L.; Saito, D. S.; Garcia, E. J.; Hart, A. J.; Villoria, R. G.; Verploegen, E. A. *Adv. Mater.* **2008**, *20*, 2707.
4. Wei, C.; Dai, L.; Roy, A.; Tolle T. B. *J. Am. Chem. Soc.* **2006**, *128*, 1412.
5. Dombovari, A.; Halonen, N.; Sapi, A.; Szabo, M.; Toth, G.; Mäkli, J.; Kordas, K.; Juuti, J.; Jantunen, H.; Kukovecz, K.; Konya, Z. *Carbon* **2010**, *48*, 1918.
6. Yao, Y.; Changhong, L.; Shoushan, F. *Nanotechnology* **2006**, *17*, 4374.
7. García, E. J.; Hart, E. J.; Wardle, B. L.; Slocum, A. H. *Adv. Mater.* **2007**, *19*, 2151.
8. Cebeci, H.; Villoria, R. G.; Hart, A. J.; Wardle, B. L. *Compos. Sci. Technol.* **2009**, *69*, 2649.
9. Marconnet, A. M.; Yamamoto, N.; Panzer, M. A.; Wardle, B. L.; Goodson, K. E. *ACS Nano* **2011**, *5*, 4818.
10. Ni, Y.; Khanh, H. L.; Chalopin, Y.; Bai, J.; Lebarny, P.; Divay, L.; VolzNi, S. *Appl. Phys. Lett.* **2012**, *100*, 193118.
11. Gong, Q.; Li, Z.; Bai, X. D.; Li, D.; Zhao, Y.; Liang, J. *Mater. Sci. Eng. A* **2004**, *384*, 209.
12. Li, L.; Yang, Z.; Gao, H.; Zhang, Z.; Ren, J.; Sun, X.; Chen, T.; Kia, H. G.; Peng, H. *Adv. Mater.* **2011**, *23*, 3730.
13. Otieno, G.; Koos, A. A.; Dillon, F.; Wallwork, A.; Grobert, N.; Todd, R. I. *Carbon* **2011**, *48*, 2212.
14. Feng, W.; Bai, X. D.; Lian, Y. Q.; Liang, J.; Wang, X. G.; Yoshino, K. *Carbon* **2003**, *41*, 1551.
15. Ravavikar, N. R.; Shadler, L. S.; Vijayaraghavan, A.; Zhao, Y.; Wei, B.; Ajayan, P. M. *Chem. Mater.* **2005**, *17*, 974.
16. Jung, Y. J.; Kar, S.; Talapatra, S.; Soldano, C.; Viswanathan, G.; Li, X.; Yao, Z.; Ou, F. S.; Avadhanula, A.; Vajtai, R.; Curran, S.; Nalamasu, O.; Ajayan, P. M., *Nano Lett.* **2006**, *6*, 413.
17. Peng, H.; Sun, X. *Chem. Phys. Lett.* **2009**, *471*, 103.
18. Pinault, M.; Mayne-L'Hermite, M.; Reynaud, C.; Beyssac, O.; Rouzaud, J. N.; Clinard, C. *Diamond Rel. Mater.* **2004**, *13*, 1266.
19. Pinault, M.; Pichot, V.; Khodja, H.; Launois, P.; Reynaud, C.; Mayne-L'Hermite, M. *Nano Lett.* **2005**, *5*, 2394.
20. Pichot, V.; Launois, P.; Pinault, M.; Mayne-L'Hermite, M.; Reynaud, C. *Appl. Phys. Lett.* **2004**, *85*, 473.
21. Pichot, V.; Launois, P.; Pinault, M.; Mayne-L'Hermite, M.; Reynaud, C.; Burghammer, M.; Riekel, C. *Elec. Prop. Novel Nanostruct.* **2005**, *786*, 158.
22. Rouzière, S.; Jourdanneau, E.; Kasmi, B.; Joly, P.; Petermann, D.; Albouy, P. A. *J. Appl. Cryst.* **2010**, *43*, 1131.
23. Pichot, V.; Badaire, S.; Albouy, P. A.; Zakri, C.; Poulin, P.; Launois, P. *Phys. Rev. B* **2006**, *74*, 245416.
24. Pichot, V. Ph.D. Thesis of University Paris Sud 11, France; **2005**.
25. Heresanu, V.; Castro, C.; Cambedouzou, J.; Pinault, M.; Stephan, O.; Reynaud, C.; Mayne-L'Hermite, M.; Launois, P. *J. Phys. Chem. C* **2008**, *112*, 7371.
26. Bouchet-Fabre, B.; Pinault, M.; Pichot, V.; Launois, P.; Mayne-L'Hermite, M.; Parent, Ph.; Laffon, K.; Durand, D.; Reynaud, C. *Diamond Relat. Mater.* **2005**, *14*, 881.
27. Castro, C.; Pinault, M.; Coste-Leconte, S.; Porterat, D.; Bendiab, N.; Reynaud, C.; Mayne-L'Hermite, M. *Carbon* **2010**, *48*, 3807.